Journal of the European Ceramic Society 20 (2000) 551–559

Microstructure and properties of monazite ($LaPO_4$) coated saphikon fiber/alumina matrix composites

K.K. Chawla[a,*], H. Liu[b], J. Janczak-Rusch[c], S. Sambasivan[d]

[a]*Department of Materials and Mechancial Engineering, University of Alabama at Birmingham, 254 BEC, 1530 Third Ave. South, Birmingham, AL 35294-4461, USA*

[b]*Sumitomo, Sitix, Albuquerque, NM 87131, USA*

[c]*EMPA Thun, Feuerwerkstrasses 39, CH-3602 Dübendorf, Switzerland*

[d]*BIRL, Northwestern University, Evanston, IL 60201, USA*

Accepted 10 August 1999

Abstract

The objective of this research was to engineer a weak interfacial bond in single crystal α-alumina (Saphikon) fiber/polycrystalline alumina matrix composites by incorporating a monazite (lanthanum phosphate, $LaPO_4$) coating onto Saphikon fibers via sol–gel dip process. Uniaxial hot pressing was used to densify $LaPO_4$-coated Al_2O_3 fiber in an Al_2O_3 matrix composites. Characterization of the composites was done by optical microscopy, SEM (scanning electron microscopy), EDS (energy dispersive spectrometer), indentation tests, three-point bend and fiber pushout tests. The results showed that the Saphikon fiber/monazite interface was weaker than the polycrystalline alumina/monazite interface. Crack deflection, interfacial debonding and fiber pullout occurred at this interface. This was attributed to the fact that the Saphikon fiber/monazite interface was smoother than the monazite/polycrystalline alumina matrix interface. Monazite coating obtained by sol–gel dip coating method withstood high fabrication temperatures (1400°C) and was conducive to the toughness properties of the composites.

Keywords: Al_2O_3 fibers; Al_2O_3 matrix; Composites; Interfaces; $LaPO_4$

1. Introduction

Ceramic matrix composites (CMCs) consisting of nonoxide fiber/nonoxide matrix, nonoxide fiber/oxide matrix or oxide fiber/nonoxide matrix are susceptible to oxidation in oxidizing environments at high temperatures, causing loss of strength and rapid decrease in toughness.[1] The degradation of properties of CMCs at elevated temperatures may be due to oxidation of the fiber, matrix, and/or interface, thermal expansion-induced residual stresses, and matrix microcracking.[2] Thus, for high temperature applications, *in air*, an oxide/oxide composite system would be desirable because of its inherent stability at high temperatures and in oxidizing atmospheres. In all composites, the interface between fiber and matrix plays a crucial role in determining the strength and toughness of the composite.[3] For instance, in a composite consisting of Al_2O_3 fiber in a SiO_2-based matrix, a strong interfacial bond (chemical bond) causes the failure mode to be similar to that of monolithic ceramics (brittle).[4] In some simple eutectic type oxide systems, such as Al_2O_3–SnO_2 and Al_2O_3–ZrO_2, no chemical reactions would be expected and these composites are relatively stable, moreover, a weak interface can change the failure mode from brittle to non-brittle.[4] In Al_2O_3/Al_2O_3 system, very strong ionic and/or covalent bonding leads to low toughness. It thus becomes necessary to apply an interface engineering approach to increase the toughness by adding a suitable interphase material between the fiber and matrix.[5]

Morgan and Marshall[6–8] investigated a number of interphase materials including simple metal oxides and mixed oxides for oxide/oxide composite systems. More significantly, for Al_2O_3/Al_2O_3 composites, they found that lanthanum phosphate, $LaPO_4$ (monazite) was a

* Corresponding author. Tel.: +1-205-934-8450; fax: +1-205-934-8485

E-mail address; kchawla@uab.edu (K.K. Chawla).

0955-2219/00/$ - see front matter
PII: S0955-2219(99)00253-8

suitable and effective oxide interphase material, which exhibited high stability at high temperature in both reducing and oxidizing environments and good chemical compatibility with alumina. They observed that the monazite/alumina fiber (Saphikon) interface had a low enough fracture resistance to satisfy the condition for interfacial debonding, when a crack grew from monazite to alumina. The monazite/alumina interface was weak enough to prevent crack growth by interfacial debonding and crack deflection. They obtained monazite coating by manually dipping Saphikon fibers in a monazite slurry, which was made by precipitation from aqueous solution with potassium phosphate. After hot pressing the Saphikon/monazite/polycrystalline alumina system at 1400 and 1600°C, minor liquid phase rich in potassium was found,[7] which was thought to cause creep at high temperatures. Kuo et al.[9] also used slurry dipping method to coat oxide fibers with monazite and studied the effect of coating thickness on the interfacial shear stress during fiber pushout.

In this work, we used a sol–gel technique to apply the monazite coatings on Saphikon fibers. Sol–gel technique is advantageous[10] because it is generally simple, it can provide better reproducibility of coating thickness and control of coating composition, and temperature of sol–gel processing is relatively low. A low processing temperature will not only reduce the cost of fabrication, but also reduce the extent of coating interaction with fibers and minimize potential coating degradation during processing. So far, some promising coating materials have been deposited uniformly on monofilament fibers and multifilament tows by sol–gel processing.[11,12] In the present work, a sol–gel dip coating method was used to coat Saphikon monofilament with monazite precursor.

The objective of this research was to use a sol–gel dip coating process to incorporate the $LaPO_4$ coating on Saphikon fibers and thus obtain a weak interfacial bond in Saphikon (single crystal α-alumina) fiber/alumina matrix composite.

2. Materials and experimental procedure

2.1. Saphikon fiber

Alpha-alumina (α-Al_2O_3) is a thermodynamically stable phase of alumina. Single crystal α-alumina fibers (trade name "Saphikon") are produced by an edge-defined film-fed jowth (EFG) technique.[13,14] The shape of the crystal is defined by the external shape of the die. This technique permits the growth of a crystal from a molten film between the growing crystal and the die. As soon as the fiber comes out of the crucible, a "size" is usually applied for ease of handling during manufacturing without damaging the surface. The size is generally a water-based emulsion coating, which can be easily washed out. For example, methyl cellulose coating is usually used on Saphikon fibers. This coating is a food grade coating that can be removed with cold water and agitation. Frequently, sinusoidal asperities have been observed on Saphikon fiber surface, which can affect both debonding and sliding abilities of this fiber within the matrix.[15] In the present work, single crystal alumina fiber with *c*-orientation, i.e. with the basal plane perpendicular to the fiber axis, was used.

2.2. Monazite precursor sol

Monazite sol was synthesized by using alcohol-based solutions of La (as lanthanum nitrate) and P (as phosphorus pentoxide) in appropriate proportions. Fibers were passed through the sol and heated to 600°C. Conversion to monazite occurred around 275°C, and heating to 600°C eliminated organic impurities. After dip coating and heat treatment, the coated fibers were embedded in alumina powder, put into a graphite die, and hot pressed at 1400°C for 1 h. The initial heating rate was 900°C per h. When the temperature reached 1400°C, a pressure of 30 MPa was applied for 1 h. The system was then allowed to cool to room temperature.

2.3. Microstructural characterization

The desized Saphikon fiber surfaces were first examined using optical microscopy and SEM. After hot pressing, the five- and 10-dip $LaPO_4$-coated Saphikon fiber/alumina matrix composites were sectioned and polished to allow the observation of microstructure of the composites. In addition, the fracture behavior, such as interfacial debonding, crack deflection and fiber pullout, was observed under SEM. Compositional analysis of the monazite coating was carried out by X-ray diffraction and energy dispersive spectroscopy (EDS).

2.4. Mechanical characterization

The ability of the monazite/alumina interfaces to exhibit interfacial debonding and crack deflection was investigated by using an indentation technique. Indentations from a Vickers hardness indentor with 9.8 N (30 s), 49 N (15 s), or 98 N (15 s) load were made in the matrix near the matrix/monazite interface, and in the fiber near the fiber/monazite interface. The indentations were oriented so that cracks from the indentation would intersect the monazite/alumina interfaces. A three-point bend test was performed to measure bend strength and test fiber pullout ability. Fiber pushout tests were also performed to measure the debonding and frictional shear stresses at the monazite/alumina interfaces.

The fiber pushout tests were performed in an in-situ SEM-pushout apparatus (Touchstone Ltd., WV). The specimens were cut and ground to a thickness between

125 and 150 μm and a finish of 0.1 μm, perpendicular to the fiber orientation. A cylindrical indentor with a 114.3 μm diameter was used to apply a load at a constant displacement rate of 0.3125 μm/s through the debonding and sliding stages.

3. Results and discussion

Fig. 1 shows the different parameters that should be considered in the precursor design of a coating. In the present case, the ethanol-based solution was clear and relatively stable. It had a low viscosity and gave a high yield of monazite (160 g/l). The monazite coating formed below 600°C. It showed good wetting and film forming characteristics. Fig. 2. shows the X-ray diffraction pattern of the coating obtained from the sol indicating the formation of stoichiometric lanthanum phosphate.

Indentation cracks, produced in the matrix with 98 N force, showed interfacial debonding. However, in the case of five-dip coating, the interfacial debonding was more clear and larger areas were debonded compared to the debonding observed in 10-dip coated composite. Fig. 3 shows that cracks passed through the alumina matrix/monazite interface and debonded the monazite/Saphikon fiber interface. Comparatively, monazite/Saphikon fiber interface was weaker than the monazite/alumina matrix interface. Fig. 4. shows two indentations made by 98 N load in the matrix on the two sides of a five-dip coated fiber. One can see smooth and continuous interfacial debonding. In Fig. 4(b) and (c), high magnification secondary electron images show clearly the crack in alumina penetrating the monazite interphase and debonding at the monazite/Saphikon fiber interface. The bright area in the backscattered electron image [Fig. 4(c)] is the monazite, which separated from the Saphikon fiber. Clearly, interfacial debonding occurred at the Saphikon fiber/monazite interface, which was less rough than polycrystalline alumina/monazite interface. This is consistent with the Morgan and Marshall analysis of interfacial debonding in this system.[7] For the 10-dip coated fiber composite, when two indentations with 98 N force were put in the matrix on the two sides of the fiber, as seen in Fig. 5, interfacial debonding was also observed. However, the crack surface was rough. It was not possible to determine which interface, if any, debonded. It is

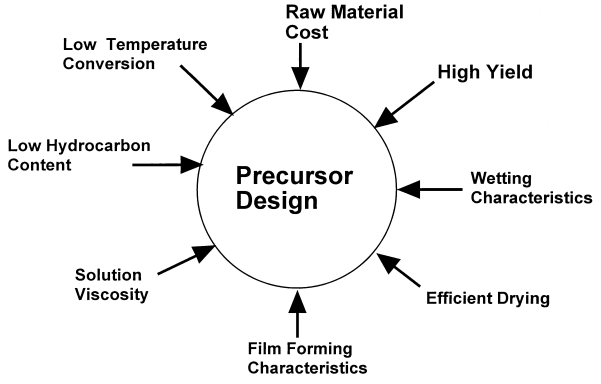

Fig 1. Various parameters to be considered in the coating precursor design.

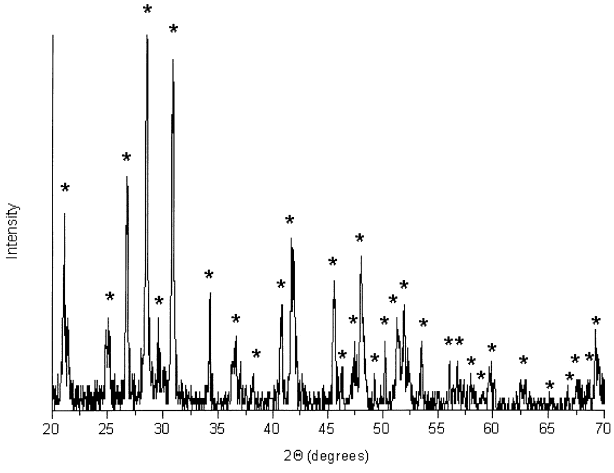

Fig. 2. X-ray diffraction pattern showing the formation of stoichiometric $LaPO_4$.

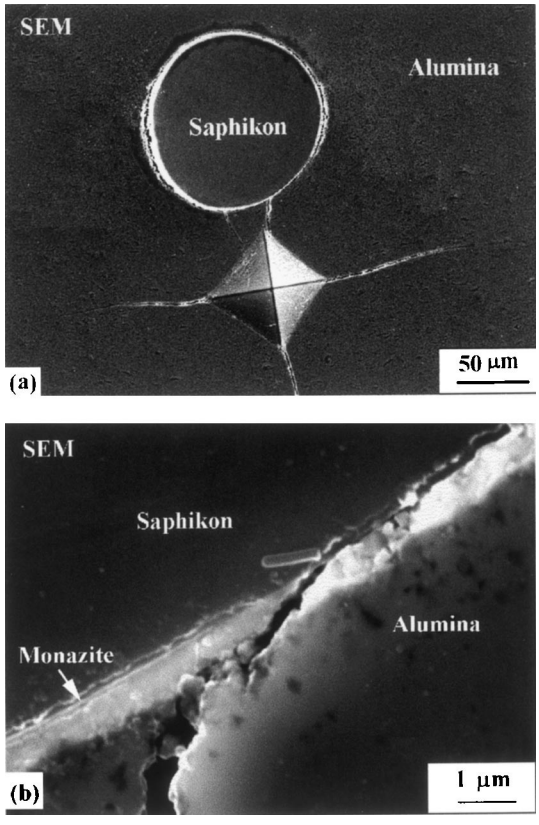

Fig. 3. Interfacial debonding at the (10-dip) monazite/Saphikon fiber interface with cracks produced by a 98 N indentation in the matrix: (a) low magnification SEM image and (b) high magnification SEM image (98 N load, 15 s). Note that cracks passed through the alumina matrix/monazite interface and debonded the monazite/Saphikon fiber interface.

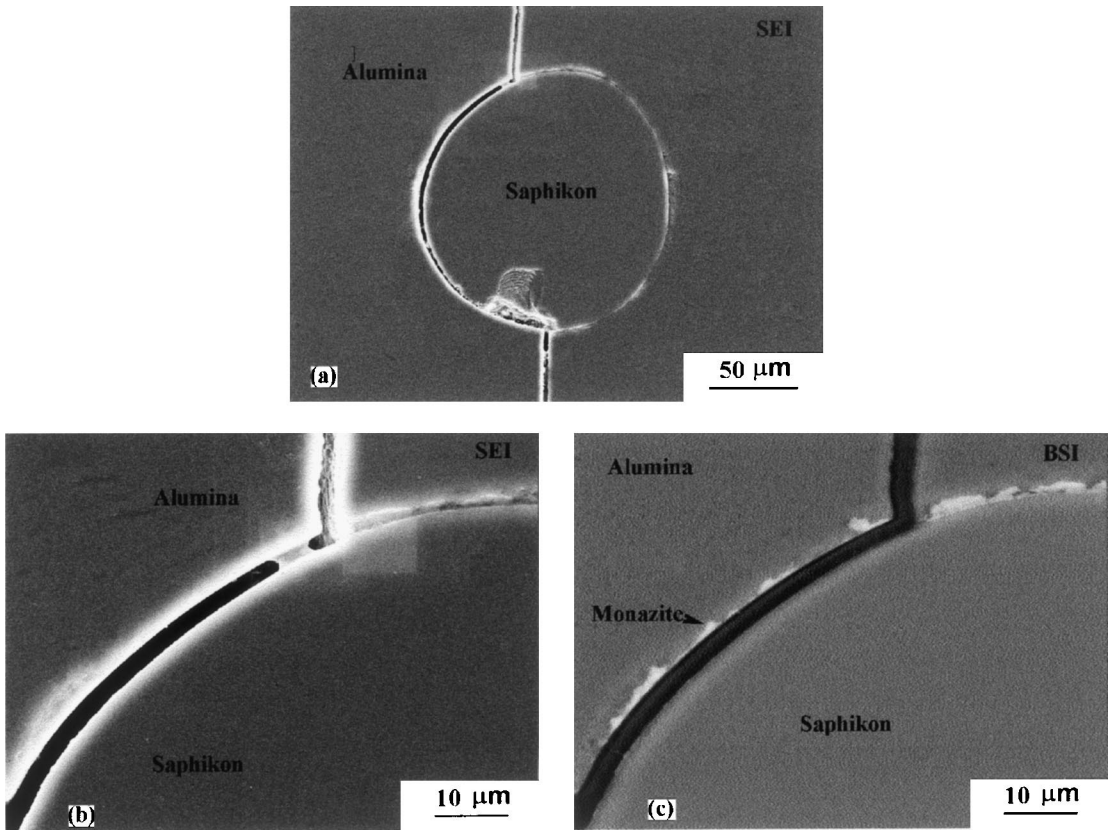

Fig. 4. Interfacial debonding at the (five-dip) monazite/fiber interface with cracks produced by two 98 N (15 s) indentations in the matrix: (a) low magnification SEI, (b) high magnification SEI, and (c) backscattered electron image of the same area shown in (b). The bright phase surrounding the Saphikon fiber is monazite. Note the interfacial debonding occurred along the Saphikon fiber/monazite interface, but not along the polycrystalline alumina/monazite interface.

just as likely that the interphase cracked, rather than separation occurring at one the two interfaces. This could be caused by the microcracking of the coating. When a Vickers indentor with a 49 N indentation was used to produce cracks in the fiber, it resulted in crack arrest, crack deflection, and interfacial debonding in five and 10-dip coated composites. Again, debonding was observed at the smooth Saphikon fiber/monazite interface but not at the rough polycrystalline alumina/monazite interface. This is contrary to the analysis of interfacial debonding due to Morgan and Marshall,[7] According to Morgan and Marshall,[7] only when a crack grew from monazite to polycrystalline alumina was interfacial debonding expected and observed, not vice versa. However, the present work showed that when cracks approached any one of the two interfaces, polycrystalline alumina/monazite or single crystal (Saphikon) alumina/monazite interfaces, interfacial debonding occurred at the smooth single crystal alumina/monazite interface rather than at the rough interface between polycrystalline alumina/monazite. It would appear that in our case, the interfacial roughness played a very important role in interfacial debonding. In spite of a certain surface roughness on the Saphikon fiber, which was grown into the fiber during manufacture and generated clamping pressures, the polycrystalline alumina/monazite interface was much rougher than the single crystal Saphikon fiber/monazite interface.

Fiber pushout tests showed that both five- and 10-dip coated fibers slid smoothly from the alumina matrix and the pushout load did not lead to matrix cracking. The shear stress–displacement curve and SEM images for a five-dip coated fiber composite with 122 μm fiber diameter and 134 μm specimen thickness are shown in Fig. 6. In Fig. 6(b), the debonded monazite coating is stuck to the matrix, i.e. the debonding occurred mostly along the Saphikon fiber/monazite interface. Fig. 7 shows the shear stress–displacement curve and SEM images for a five-dip coated fiber composite with 163 μm fiber diameter and 145 μm specimen thickness. A sinusoidal variation in the shear stress–displacement curve can be seen. This was probably caused by sinusoidal asperities existing on the fiber surface.

A comparison of pushout shear stress/displacement curves of five- and 10-dip coated composites showed that the five-dip coated composites debonded at higher shear stress values than the 10-dip coated composites, and also the frictional shear stress in these composites was higher. The reasons are as follows. Debonding usually involves a Mode II (shear) fracture phenomenon.

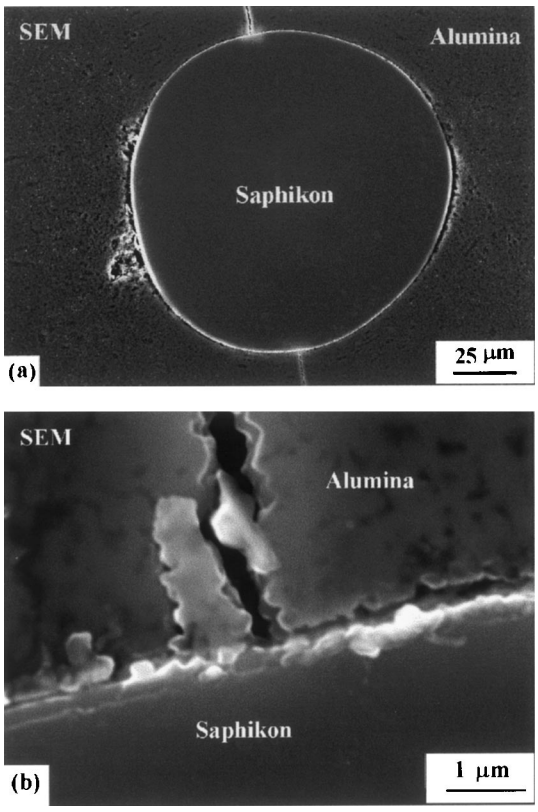

Fig. 5. Interfacial debonding at the (10-dip) monazite/fiber interface with cracks produced by two 98 N (1 5 s) indentations in the matrix; (a) low magnification SEM image and (b) high magnification SEM image. Note the roughness of the debonded fracture surface.

In brittle systems, Mode II fracture typically occurs by the coalescence of microcracks in a layer. In the case of a thick coating, the 10 dip coating in the present case, this layer coincides with the coating itself such that debonding involves a diffuse zone of microcrack damage. In other cases, the layer is very thin and the debond has the appearance of a single crack. A schematic of the interfacial debonding models for thin and thick interphase is shown in Fig. 8. The 10-dip coating may have some defects in it, making it easier to form microcracks in the coating itself and debonding may occur by the coalescence of microcracks within the monazite coating. The coefficient of friction in the fractured monazite is likely to be higher than that of monazite/Saphikon interface with a thinner coating (five-dip), where initiation of debonding occurs by a single crack along the Saphikon fiber/monazite interface.

The stress–displacement curves in three-point bend tests at room temperature of five-dip fiber coated composites and monolithic alumina are shown in Fig. 9. The composite failed in a non-brittle manner. The load increased until a stress of about 180 MPa, where the fibers started to debond and pullout from the matrix. After debonding and pullout, the matrix still could transfer some load. Finally, the ultimate stress (~230 MPa) was reached. There, the stress suddenly decreased

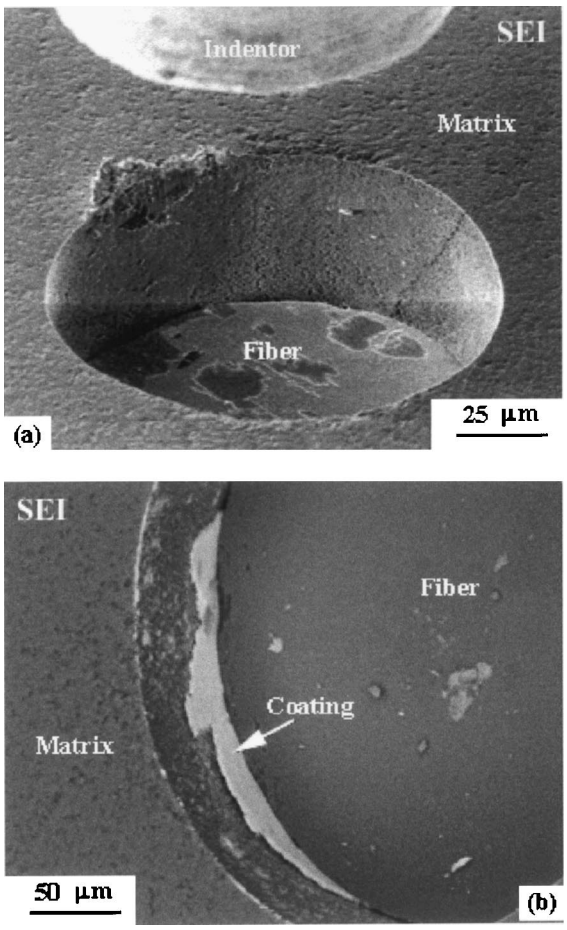

Fig. 6. Fiber pushout test results on a Saphikon/five-dip $LaPO_4/Al_2O_3$ composite with 122 μm fiber diameter and 134 μm specimen thickness: (a) SEM image showing the debonded fiber is pushed out of the alumina matrix, (b) SEM image showing the debonded monazite coating is stuck to the matrix.

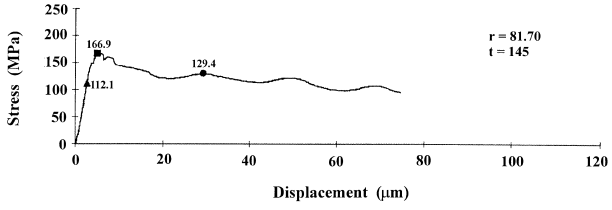

Fig. 7. Shear stress–displacement curve for a Saphikon/five-dip $LaPO_4/Al_2O_3$ composite with 163 μm fiber diameter and 145 μm specimen thickness. Note a sinusoidal variation in the curve which corresponds to the asperities on the as-received fiber surface.

when the matrix failed. The monolithic alumina failed catastrophically; its bend strength was very low (~140 MPa). Comparatively, the work of fracture of monazite coated Saphikon fiber/alumina matrix composites is much higher than that of monolithic alumina. Note that the fiber volume fraction in the composite was very small, about 0.01. The fracture surfaces of five-dip specimens fiber pullout was observed and the average length of pullout fiber was about 130 μm. In most cases, the monazite coating was largely peeled off the fiber.

3.1. Interfacial Roughness

The degree of interfacial roughness is a very important factor in a mechanically bonded interface.[2] A very large interfacial roughness usually results in strong mechanical keying, which can prevent interfacial debonding and fiber pullout, while a smooth interface leads to weak keying, which is desirable for fiber pullout. Many investigators[15–18] studied interfacial roughness and found that interfacial roughness had a

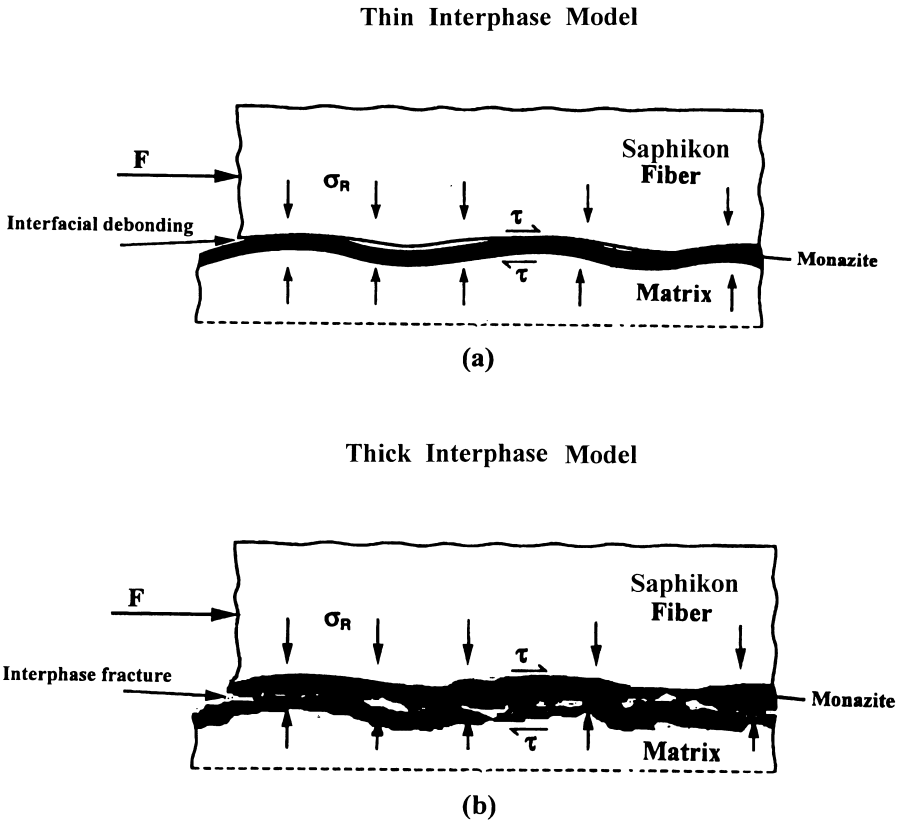

Fig. 8. Schematic of the interfacial debonding models for thin and thick interphase: (a) thin interphase model wherein debonding occurs by a single crack along the Saphikon fiber/monazite interface; (b) thick interphase model wherein debonding occurs by the coalescence of microcracks within the monazite coating.

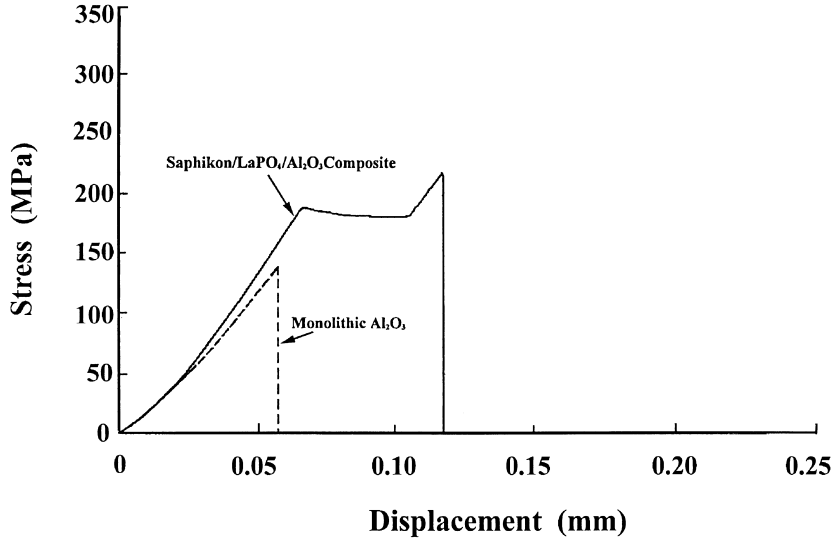

Fig. 9. The stress–displacement curves of a five-dip composite and monolithic alumina in a three-point bend test at room temperature. Note that the fiber volume fraction in the composite was very small, about 0.01.

pronounced effect on the interfacial sliding stress. Mackin et al.[15] observed sinusoidal modulations in the load–displacement curves of Saphikon/glass and Saphikon/γ-TiAl composites identical in wavelength to the surface roughness of the Saphikon fibers. Parthasarathy et al.[18] found that sliding resistance increased with the radial clamping stress by an amount proportional to A/r, where A is the amplitude of the roughness and r the fiber radius. The roughness amplitude of Saphikon fibers, A, measured by atomic force microscopy (AFM) is 0.0077 μm.[4] The fiber radius r used in the present work is around 70 μm, therefore the interfacial roughness

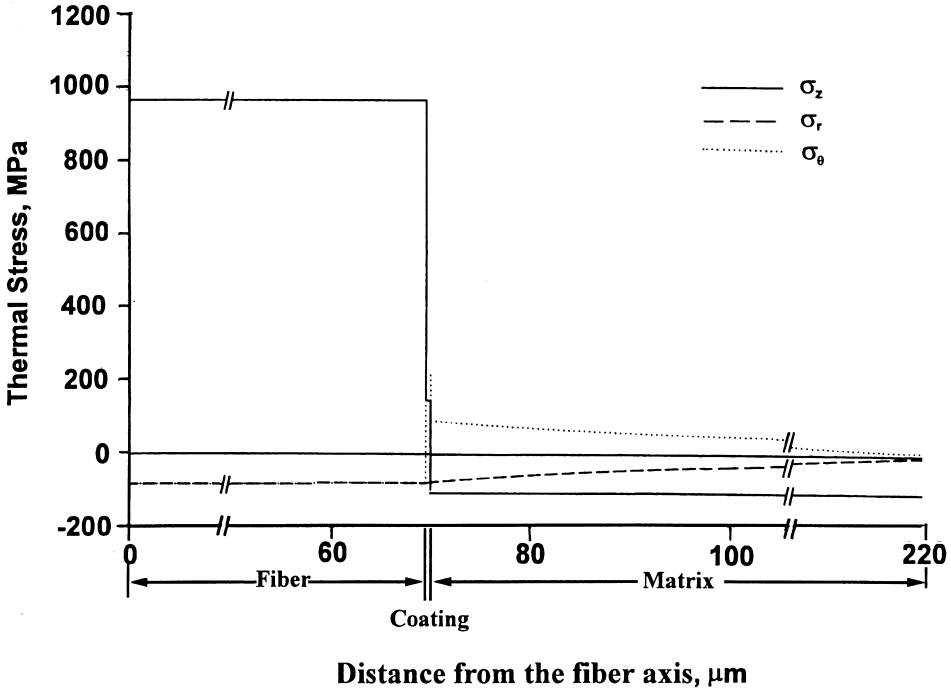

Fig. 10. Thermal stresses in a Saphikon/five-dip monazite/alumina composite, where $V_f = 0.01$ and $\Delta T = 1000°C$. The coating thickness is 0.5 μm.

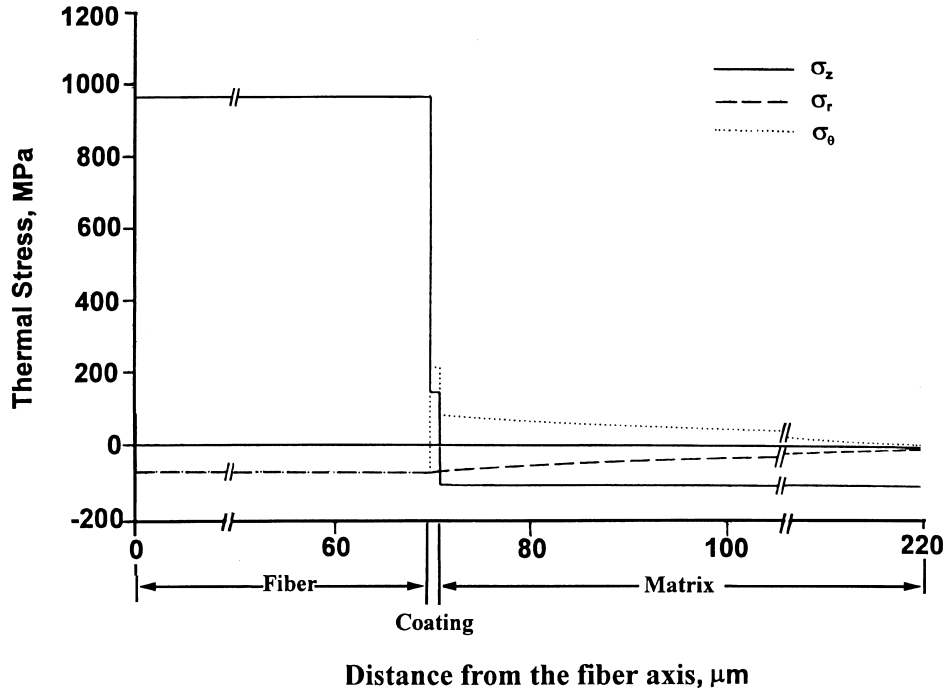

Fig. 11. Thermal stresses in a Saphikon/10-dip monazite/alumina composite where $V_f = 0.01$ and $\Delta T = 1000°C$. The coating thickness is 0.5 μm.

strain A/r is about 0.00011. Thermal strain $\Delta\alpha\Delta T$ in Saphikon/monazite interface is equal to 0.0008 if $\Delta T = 1000°C$. Comparatively, the thermal strain is about 8 times greater than the roughness-induced strain. Thus, the effect of interfacial roughness of monazite/Saphikon fiber would not be significant. Specifically, when compared with that of monazite/polycrystalline alumina, the roughness-induced radial clamping strain at the monazite/Saphikon interface is very small.

3.2. Thermal stress analysis

We used a three-layer model[2] to calculate the thermal stresses for the five- and 10-dip coated composites, respectively. A 0.01 fiber volume fraction we used a 1000°C temperature change and 0.5 and 1 μm coating thickness for five- and 10-dip, respectively. The distribution of thermal stresses in Saphikon fiber/$LaPO_4$/alumina, matrix composite for two coating thicknesses is shown in Figs. 10 and 11. The difference between the two figures is insignificant. One can see that all the stress components are constant in the central fiber. The σ_z is constant in the coating as well as the matrix. The σ_θ is discontinuous at the interface. The σ_r maintains continuity at the interface, and goes to zero at the free surface. This analysis shows radial gripping increased the strength of the fiber/monazite and monazite/matrix interfaces. However, the magnitude of the thermal radial stress is low and gripping due to thermal stress is not significant. The total radial stress is the sum of the thermal stress and the stress due to the interfacial roughness.[2] The roughness-induced radial stress is much greater at the monazite/polycrystalline alumina interface than at the single-crystal alumina/monazite interface, although they are both mechanically bonded. This probably is the reason why debonding occurred more often at the fiber/monazite interface instead of the monazite/matrix interface.

The present work has demonstrated the effective interface engineering approach by sol–gel dip coating method. There are, however, some unanswered questions. A detailed study on the coating thickness effects on the debonding behavior is necessary. More uniform coating thickness should be obtained. Measurements of interface shear stress as a function of thickness should be done in a systematic manner. We also recognize that very low fiber volume fraction was used in present work (0.001) due to the high cost of the single-crystal alumina fiber and small amount of monazite precursor sol. We suggest increasing fiber volume fraction and decreasing fiber diameter to create statistically better measurements. One practical way is to use Nextel™ 610 oxide alumina fibers instead, which are less expensive. Also, because of the ambiguous estimates of interfacial energy for $LaPO_4$/Al_2O_3 interface and for $LaPO_4$/single crystal Al_2O_3, future work to measure these values would be useful.

4. Conclusions

From the results and discussions presented in this present work, we can make the following conclusions:

1. The incorporation of monazite interphase coating by sol–gel dip coating method is an effective way of creating weak interfacial bonds between monazite and alumina.
2. Two-phase layered liquid dipping method for coating monofilament Saphikon fibers with monazite sol was effective.
3. The presence of monazite as an interphase was successful in providing weak interface to both single-crystal alumina and polycrystalline alumina.
4. The roughness-induced clamping was much greater at the rough monazite/polyerystalline alumina interface as compared with the smooth single crystal alumina/monazite interface. Therefore, the Saphikon fiber/monazite interface was relatively weak and interfacial debonding and fiber pullout were easier to initiate at this interface than at the polycrystalline alumina/monazite interface. It did not matter in which phase the crack originated.
5. A sinusoidal variation in the five-dip shear stress–displacement curve due to the sinusoidal asperities on fiber surface was observed.
6. The energy expended in interfacial debonding leading to fiber pullout caused an increase in toughness or work of fracture of such composite materials.
7. Thermal stress analysis showed radial gripping, which increased the strength of the interfaces. However, the magnitude was not significant because of the small thickness of coating.

References

1. Prewo, K. M. and Batt, J. A., The oxidative stability of carbon fiber reinforced glass-matrix composites. *J. Mater. Sci.*, 1988, **23**, 523–527.
2. Chawla, K. K., *Ceramic Matrix Composite*. Champion and Hall, London, 1993.
3. Chawla, K. K., *Composite Materials*, 2nd ed. Springer Verlag, New York, 1998.
4. Chawla, K. K., Ferber, M. K., Xu, Z. R. and Venkatesh, R., Interface engineering in alumina/glass composites. *Materials Science and Engineering*, 1993, **A 162**, 35–44.
5. Chawla, K. K., Schneider, H., Schmücker, M. and Xu, Z. R. in *Processing and Design Issues in High Temperature Materials*, TMS, Warrendale, PA, 1997, pp. 235–245.
6. Morgan, P. E. D. and Marshall, D. B., Functional interfaces for oxide/oxide composites. *Mater. Sci. Eng.*, 1993, **A162**, 15–25.
7. Morgan, P. E. D. and Marshall, D. B., Ceramic composites of monazite and alumina. *J. Am. Ceram. Soc.*, 1995, **78**, 1553–1563.
8. Morgan, P. E. D., Marshall, D. B. and Housley, R. M., High-temperature stability of monazite–alumina composites. *Mater. Sci. Eng.*, 1995, **A195**, 215–222.

9. Kuo, D.-H., Kriven, W. M. and Mackin, T. J., Control of interfacial properties through fiber coatings: monazite coatings in oxide–oxide composites. *J. Am. Ceram. Soc*., 1997, **80**, 2987–2996.
10. Reed, J. S., *Principles of Ceramics Processing*. John Wiley, New York, 1988.
11. Hay, R. S. and Hermes, E. E., Sol–gel coatings on continuous ceramic fibers. *Ceram. Eng. Sci. Proc*., 1990, **11**, 1526–1538.
12. Villalobos, G. R. and Speyer, R. F., Glass-ceramic sol gel coating of ceramic fibers. *Ceram. Eng. Sci. Proc*., 1994, **15**, 731–742.
13. Labelle, H. E., Growth of controlled profile crystals from the melt. *Mater. Res. Bull*., 1971, **6**, 566–581.
14. Chawla, K. K., *Fibrous Materials*. Cambridge Unviersity Press, Cambridge, UK, 1998.
15. Mackin, T. J., Yang, J. and Warren, P. D., Influence of fiber roughness on the sliding behavior of sapphire fibers in TiAl and glass matrices. *J. Am. Ceram. Soc*., 1992, **75**, 3358–3362.
16. Jero, P. D., Kerans, R. J. and Parthasarathy, T., Effect of interfacial roughness on the frictional stress measured using pushout tests. *J. Am. Ceram. Soc*., 1991, **74**, 2793–2801.
17. Venkatesh, R. and Chawla, K. K., Effect of interfacial roughness on fiber pullout in alumina/SnO_2/glass composites. *J. Mater. Sci. Lett*., 1992, **11**, 650–652.
18. Parthasarathy, T. A., Barlaye, D. R., Jero, P. D. and Kerans, R. J., Effect of interfacial roughness parameters on the fiber pushout behavior or a model composite. *J. Am. Ceram. Soc*., 1994, **77**, 3232–3236.